

# Multiple type discriminating mine fire sensors

J.C. Edwards, R.A. Franks, G.F. Friel, C.P. Lazzara and J.J. Opferman

Research physicist, electronics engineer, chemical engineer, physical scientist and electronics technician, respectively, NIOSH/Pittsburgh Research Laboratory, Pittsburgh, Pennsylvania

## Abstract

*It was determined that a selection of different types of fire sensors could be used to discriminate mine fires from nuisance emissions produced by diesel equipment. A neural network (NN) was developed for application to coal, wood and conveyor-belt fires in the presence of diesel emissions and was evaluated with the successful prediction of 22 out of 23 mine fires based on a fire-probability determination. The optimum sensor selection for the NN was comprised of a carbon monoxide (CO) sensor, two types of metal oxide semiconductor (MOS) sensors and an optical path smoke sensor.*

## Introduction

Miner safety can be jeopardized by mine fire detector response to nuisance emissions from diesel equipment, torch cutting and welding activities. These emissions include carbon monoxide (CO) and smoke particulates, which are common open-fire signatures. In the absence of nuisance emissions, a CO sensor has a good record for mine fire detection, with some exceptions. For example, fire tunnel experiments (Hambleton et al., 1997) for a range of fuels demonstrated that electrochemical cell CO sensors did not have the sensitivity for early detection of smoldering coal dust and conveyor belt fires. For a flaming conveyor belt, the CO sensor had a large response. These experiments also showed the inadequacy of an ionization smoke sensor for smoldering fires. Multiple sensor technologies were recommended for mine fire detection. Although MOS sensors are very sensitive to products of combustion (POC), they are not very selective. Multiple sensor types, which include electrochemical cell CO sensor and MOS sensors, were shown in laboratory coal studies (Brinn and Bott, 1994) to be a significant improvement for coal heating detection at low temperatures. They showed that a neural network could be used to differentiate shot firing from fire sources.

Neural network approaches to fire recognition in the presence of nuisance emissions with multiple-type fire sensors have been used in nonmining applications. The advantage of a neural network approach is its capability to classify an event based on multiple-type sensors' response to various signatures. A neural network approach is very useful for nonlinear sensor responses. One approach (Ishii et al., 1994) to fire detection and nuisance signal discrimination applied a neural network to heat, smoke and CO generation rates, and their temporal differentials, derived from the measured temperature, smoke extinction coefficient and CO concentration. More recently, Rose-Pehrsson et al., 2000, demonstrated with

five sensors that a multivariate analysis could classify various fire sources from nuisance emissions.

Mining applications (Edwards et al., 2001, 2002) have extended Brinn and Bott's (1994) approach with the inclusion of additional sensors for early detection and nuisance signal discrimination capability. It was determined (Edwards et al., 2001) from combustion detection experiments conducted in the Safety Research Coal Mine (SRCM) at the National Institute for Occupational Safety and Health (NIOSH) Pittsburgh Research Laboratory (PRL) that an ionization smoke sensor, an optical smoke sensor and metal oxide semiconductor (MOS) sensors, with an alarm point defined as a ten standard deviation change in the sensor signal from the signal's ambient, alarmed prior to an electrochemical CO sensor's detection of 5 ppm CO concentration. This was particularly important for a smoldering conveyor belt that produced visually obscuring smoke in the absence of CO production. The combustibles included coal, electrical cable insulation, conveyor belt and diesel fuel.

The capability of multiple sensor types to discriminate smoldering coal and conveyor belt combustion from diesel emissions was demonstrated (Edwards et al., 2002) with mine fire experiments in the presence of diesel emissions. It was determined that either a nitric oxide ( $\text{NO}_x$ ) sensitive MOS sensor or a ratio of normalized ionization smoke sensor signal to normalized optical smoke sensor signal could provide the nuisance signal discrimination. It was also demonstrated that not only would an ionization smoke sensor discriminate battery charging from the false response of the chemical cell CO sensor to hydrogen ( $\text{H}_2$ ) produced by the battery charging operation, but, in conjunction with a  $\text{NO}_x$ -sensitive MOS sensor, it could discriminate smoldering to flaming coal combustion transition from diesel emissions (Edwards et al., 2001).

A NN was trained to discriminate coal and belt combustion in a diesel emissions background based on a CO sensor, a

Nonmeeting paper number 03-312. Original manuscript submitted for review April 2003. Revised manuscript received and accepted for publication October 2003. Discussion of this peer-reviewed and approved paper is invited and must be submitted to SME Publications Dept. prior to Sept. 30, 2004.

NO<sub>x</sub>-sensitive MOS sensor and an optical sensor (Friel et al., 2002). The fire alarm for these cases was defined as the increase in the neural network fire probability above 0.5. Because combustion increased once initiated, the probability continued to increase asymptotically to approximately 0.95 with time. The 0.5 criterion triggered the fire alarms to occur within ten minutes after the first visual smoke observation for thirteen data sets.

To extend the range of validity of the multiple-type fire sensor and neural network approach to early and reliable mine fire detection, it is necessary to expand the number of combustible sources for the neural network training data set. The optimum neural network for mine fire in the presence of diesel emissions prediction requires a representation of as many expected mine fire combustible sources as possible. For this purpose, additional research was conducted at PRL to evaluate the sensors' fire detection capability for wood fires in the presence of diesel emissions. The neural network analysis was extended to include training data sets constructed from coal, conveyor belt and wood fires in the presence of diesel emissions and in the absence of diesel emissions. The optimum selection of sensor types for mine fire detection was based upon the neural network's best prediction of a mine fire with these three mine fire sources.

### Mine fire experiments

To supplement the previous coal and belt fire detection experiments (Edwards et al., 2002) that were conducted in the SRCM for applications to the development of a neural network for mine fire nuisance signal discrimination, a series of wood-fire detection experiments were conducted in the SRCM. The sensors used in the evaluation are listed in Table 1. These sensors include:

- M1, a metal oxide semiconductor (MOS) sensor that is responsive to POC hydrocarbons, CO and H<sub>2</sub>;
- M2, a MOS sensor that exhibits a bimodal response to NO<sub>x</sub> and POC;
- CO, an electrochemical cell carbon monoxide sensor;
- SA, an infrared optical path-smoke sensor with a 9-m (30-ft) path length; and
- SB, an ionization smoke sensor.

The CO sensor was manufactured by Conspec Controls Inc; the MOS sensors by Figaro USA Inc; sensor SA by Detection Systems Inc; and sensor SB by Anglo American Electronics Laboratory<sup>1</sup>. The CO sensor, which has a maximum range of 50 ppm, was calibrated with 25 ppm CO in hydrocarbon-free air.

The MOS sensors' response to gas emissions are based on the principle of reduced current flow through the heated sensor element when O<sub>2</sub> is absorbed on the element surface and the sensing surface element's electrical resistance increases. The presence of a deoxidizing POC gas will be detected through a reduction in the sensor surface resistance, which is directly measured as a voltage change across a load resistor in a voltage divider. The net effect is that the output voltage measured across the load resistor in series with the sensor element resistance is inversely proportional to the sensor resistance. In response to NO<sub>x</sub>, the bimodal sensor M2 responds to additional O<sub>2</sub> with an increase in the sensor element's surface resistance.

<sup>1</sup>Mention of any company does not constitute endorsement by NIOSH.

**Table 1 — Sensors for POC-nuisance emissions evaluation.**

Sensor	Type
CO	Chemical cell
SA	Optical smoke
SB	Ionization smoke
M1	MOS (POC)
M2	MOS (bimodal NO <sub>x</sub> - POC)

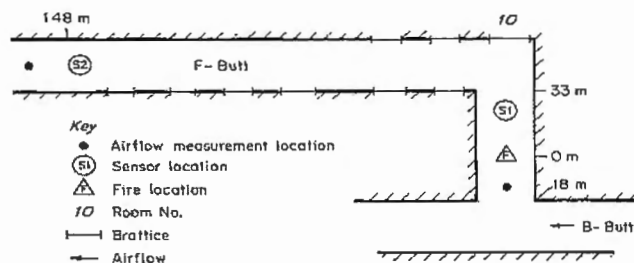


**Figure 1 — Plan view of SRCM section.**

Figure 1 shows the location of the fire and sensor stations in a section of the SRCM. Sensor station S1 is 18 m (60 ft) downwind from the fire, and station S2 is 148 m (485 ft) downwind from the fire. Room 10 has an average height and width of 2.0 and 3.9 m (6.6 and 12.8 ft), respectively. F-Butt has an average height and width of 1.9 and 4.5 m (6.2 and 14.7 ft), respectively. The dispersion and dilution of POC associated with the airflow from S1 to S2, and the leakage around crosscut brattices, resulted in the classification of each experiment into two experiments for the purpose of analysis associated with sensor responses at S1 and S2. For those experiments with a diesel emissions background, a diesel locomotive was positioned in B-Butt at its intersection with Room 10 to supply diesel emissions to the airflow in Room 10. For the wood-combustion experiments, the diesel locomotive emissions were fed directly into Room 10, as was the case for the belt combustion experiments.

The locomotive was positioned in B-Butt upwind of Room 10 for the coal combustion experiments. The coal and belt fuel sources were described previously (Edwards et al., 2002). In each wood combustion experiment, 460-mm- (18-in.-) long-oak sticks, approximately 16 by 16 mm (0.63 by 0.63 in.) in cross section cut from mine support timber, were placed parallel to each other in two mutually orthogonal layers with seven sticks in each layer to form a small crib structure. There was an air gap of one stick width between any two adjacent sticks.

The wood crib was placed on a 0.61-m- (2-ft-) square steel plate, which was heated on its bottom surface by electrical strip heaters. The total wood mass was approximately 2.4 kg (5.3 lb). The average heating rate was 1.6 kW. Figure 2 shows the sensor array at S1, approximately 18 m (60 ft) downwind from the fire location. The light obscuration monitor is used to determine the smoke optical density. Sensor station S2, 148 m (485 ft) downwind from the fire location, has a duplicate set of sensors.

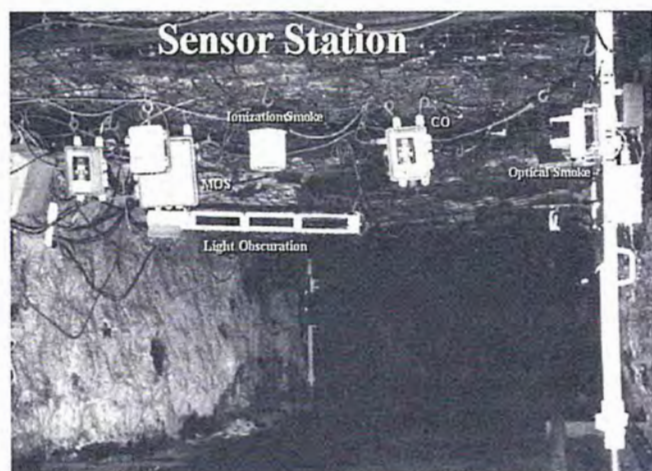


Figure 2 — SRM mine fire sensors at S1.

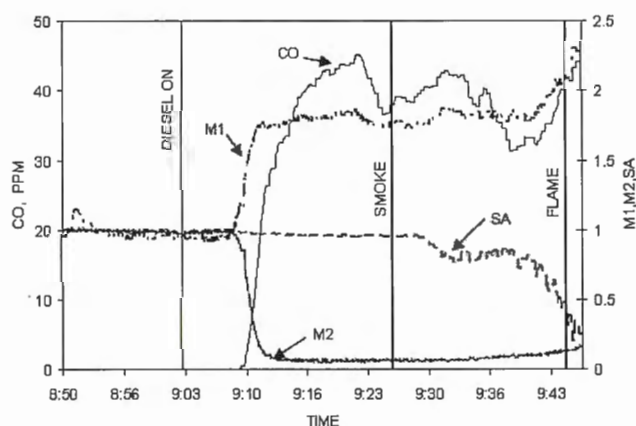


Figure 3 — Sensor responses at S1 for wood fire in presence of diesel emissions.

## Results

**Sensor response.** Figure 3 shows the responses of sensors M1, M2, CO and SA at Station S1 to a wood fire in the presence of diesel emissions for experiment T82S1. T82S1 refers to experiment Number 82 measurements at Station S1. The experiments are identified by combustion source and presence of diesel emissions in Table 2. The response values of the sensors were normalized by their ambient prediesel emissions background, except for the CO sensor from which the ambient value was subtracted. Only the optical smoke sensor SA was not affected by the diesel emissions. SA responds to the smoldering and flaming wood combustion. Sensors M1, M2 and CO were significantly affected by the diesel emissions, but showed a less significant response to the smoldering wood fire POC than did the optical smoke sensor, SA. For the same experiment, Fig. 4 shows that the response of the ionization smoke sensor, SB, to the diesel emissions is significant, in contrast to the response of SA shown in Fig. 3. The significant departure from the previous coal and belt experiments (Edwards et al., 2002) is the absence of a recovery in MOS Sensor M2 to a value above ambient when exposed to wood-fire POC. This is a function of the proportionally greater concentration of  $\text{NO}_x$  from diesel emissions than wood combustion POC. For the experiments conducted

Table 2 — Summary of SRM mine fire experiments.

Experiment No./Sensor station	Combustible	Diesel emissions	Flow, $\text{m}^3/\text{s}$	Flow Ratio
T71S2	Coal	no	4.3	1.7
T74S1	Coal	yes	2.7	
T74S2	Coal	yes	5.4	2.0
T75S1	Coal	yes	2.0	
T75S2	Coal	yes	3.9	1.9
T76S1	Coal	yes	3.3	
T76S2	Coal	yes	4.2	1.3
T77S1	Belt	yes	3.3	
T77S2	Belt	yes	5.7	1.7
T78S1	Belt	yes	1.9	
T78S2	Belt	yes	3.8	2.1
T79S1	Belt	yes	2.8	
T79S2	Belt	yes	5.4	1.9
T81S1	Wood	no	1.7	
T81S2	Wood	no	3.5	2.1
T82S1	Wood	yes	2.1	
T82S2	Wood	yes	4.8	2.3
T83S1	Wood	yes	2.9	
T83S2	Wood	yes	2.8	1.0
T84S1	Wood	yes	3.1	
T84S2	Wood	yes	4.5	1.4
T85S1	Belt	no	3.1	
T85S2	Belt	no	4.2	1.4

during the smoldering stage, the wood-fire CO production appeared to approach the flaming mode with a growth quadratic in time, in contrast with the linear CO production rate associated with the smoldering belt and coal experiments. Figure 5 shows the response of sensors CO, M2 and SA to coal combustion in the presence of diesel emissions for experiment T76S1. In this experiment, the CO delivered by the diesel is about one-tenth of the CO delivered by the diesel in wood-combustion experiment T82S1 shown in Fig. 3. Consequently, the  $\text{NO}_x$  is reduced proportionally, and sensor M2 recovers above its ambient value in response to the POC in contrast with the wood-combustion experiment.

The ratio of the ionization smoke sensor normalized response to the optical smoke sensor normalized response showed a decrease below its ambient clear air value in the presence of diesel emissions, followed by an increase above ambient in the hazardous combustion period. The response of this ratio at S1 is shown in Fig. 4. This pattern was consistent for all the wood combustion experiments, with the exception of T83S2, for which the POC dilution was too extensive. Similarly, this pattern was observed for the coal and conveyor belt fire detection experiments (Edwards et al., 2002), although for those cases the ratio exceeded the clear air ambient value earlier in the smoldering combustion stage.

**Neural network analysis.** Responses of the different sensor types to various fire signatures are not individually capable of distinguishing a fire from nuisance diesel emissions. Because various fire sources can have distinct emission signatures, it most likely is not possible to distinguish a fire from nuisance emissions without the deployment of multiple sensor types. One method to incorporate the results of multiple-type fire sensors is to use a neural network approach. A neural analysis method is used to classify events based upon a training set of

known events. The neural network selected (NeuroSolutions from NeuroDimension Inc.) for this analysis was a two hidden layer neural network (NN) with 20 process elements (PE) in the first layer and ten process elements in the second layer. This selection was based on the optimum prediction with the training data. Each process element used a hyperbolic tangent function activation function that operated on the linear combination of inputs to the PE.

The neural network was trained on a data set with constituent inputs representative of the sensor data to be collected with the atmospheric mine monitoring system. The inputs to the neural network are measurable sensor data and selected products of data values. The selection of input sensor-type data was determined by trial and error to optimize the classification of clear air, diesel emissions and fire. As a result of the trial-and-error approach to predict the occurrence of a fire, the set of sensors CO, M1, M2 and SA were found to be the optimum choice. In addition to the normalized sensor data from the four selected sensors, it was determined that the optimum fire prediction occurred with the inclusion in the input set the product combinations M1 X M2 and CO X SA.

The training set data files, T71S2, T75S1, T79S1, T81S1, T82S1 and T85S1, included each of the coal, belt and wood combustibles with and without diesel emissions background. For the coal and belt combustion training set experiments, the diesel emissions were delineated from clear air when sensor M2 decreased ten standard deviations below the clear air ambient, and the fire POC were delineated from diesel emissions background when sensor M2 increased ten standard deviations above the clear air ambient value. Because of the weak response of M2 to the wood fires in the presence of diesel emissions, the wood fire POC were delineated from diesel emissions background by the response of the optical smoke sensor SA.

The experimental results at S1 and S2 were differentiated by the dilution and dispersion of the POC and diesel emissions. The dilution was significantly affected by the leakage into F-Butt around the brattices shown in Fig. 1. Table 2 shows the volumetric airflow at S1 and S2, and the ratio of airflow at S2 to that at S1 for the experiments. The average increase in airflow was 70%. Once the neural network is trained, the application can proceed to the prediction of the fire probability. The agreement of the predicted fire probability with the visual observation of smoke from the fire is a measure of a successful neural network prediction.

The application of the neural network program developed from the training data set to the 23 training and testing data sets listed in Table 2 yielded a set of fire-probability curves. Predicted fire probability curves for a wood and coal fire in the presence of diesel emissions are shown in Figs. 4 and 5. The figures show good agreement between the visual observation of smoke and the significant increase in the predicted fire probability. The criterion established for recognition of a fire by the neural network program corresponds to the probability equal to 0.5. This follows from the three possible classifications of clear air, nuisance emissions and fire and from the fact that the probability of each of the other events will be less than 0.5 if the fire probability is greater than 0.5.

The optical density at which the probability curve indicated a fire was  $0.0074 \text{ m}^{-1}$  for the coal fire and  $0.013 \text{ m}^{-1}$  for the wood fire, respectively. The smoke optical density was determined from the light obscuration monitor at the sensor station. This measurement of optical density included the background diesel emissions. These values are less than the  $0.022 \text{ m}^{-1}$  optical density defined to be the alarm value for a

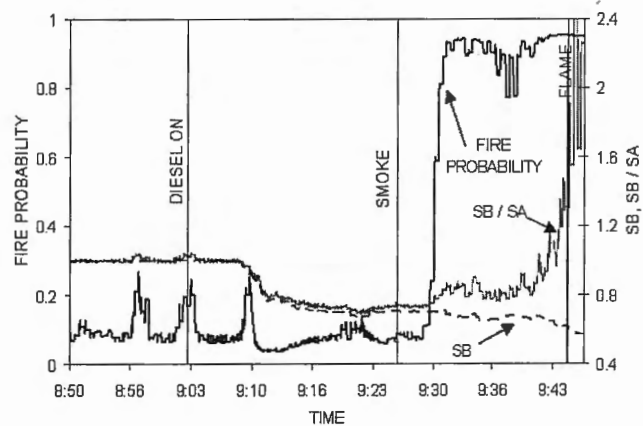


**Figure 4**—Response of ratio of ionization sensor response to optical sensor response for wood fire in presence of diesel emissions.

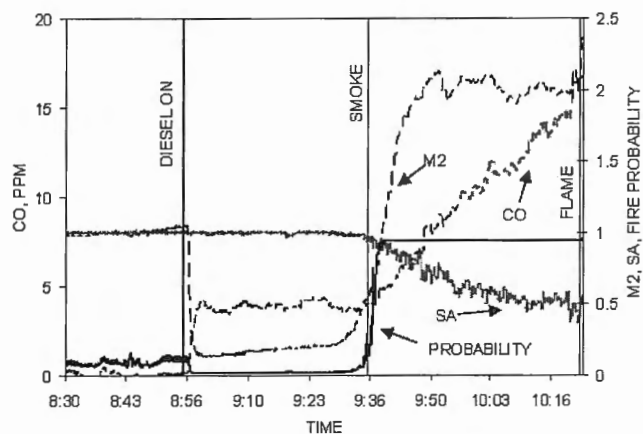


**Figure 5**—Sensor response at S1 for coal fire in presence of diesel emissions.

mine smoke sensor (Code of Federal Regulations, 2001). Figure 4 also shows that the neural network fire prediction is earlier than the indication of a fire from the ratio of the ionization smoke sensor response to the optical smoke sensor response. For all the experiments conducted, the NN fire prediction is no later than the indication of a fire by this ratio. The noise inherent in this ratio of signals makes it difficult to be used as a defined fire alarm point.

For the 23 experiments conducted, the fire probability indicated a fire in 22 of the experiments and the average optical density at a fire probability of 0.5 was  $0.0057 \text{ m}^{-1}$ . In only one experiment, T83S1, did the optical density exceed  $0.022 \text{ m}^{-1}$  when the fire probability equaled 0.5, and in that particular wood-fire in the presence of diesel emissions experiment, the optical density was  $0.023 \text{ m}^{-1}$ . The fire probability alarm relative to first observation of smoke at S1 and S2 is displayed as a radar chart in Fig. 6. The smoke observation is set to time zero. Each concentric circle on the chart represents 20 min elapsed time, with the smoke referenced at time zero. Detection of signatures from the smoke and flame occurrences at S1 were based upon visual observations. The average estimated travel time from the fire to S1 was one minute for all the experiments. Because of the uncertainty in the visual observations and the fluctuations in the airflow, this

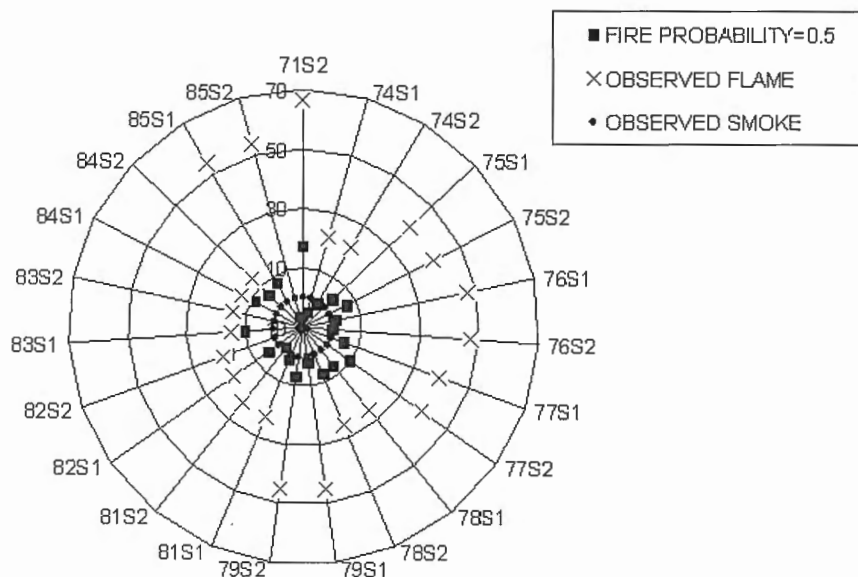


**Figure 6**—Summary of neural network fire prediction relative to observed smoke and flame.

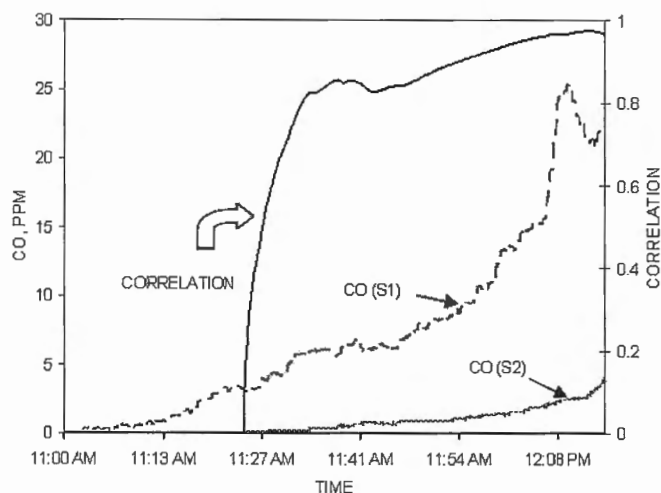


**Figure 7**—Correlation between measured CO from belt combustion at sensor stations 130 m (427 ft) apart.

time difference was ignored. Determination of the arrival of smoke and flame POC at S2 were projected from the transport time between S1 and S2 as defined by the time lag of the first detection of CO at the stations. With the exception of T83S2, the NN predicted fire alarm occurred prior to flaming combustion. The absence of an alarm for T83S2 was due to the dilution of the POC at S2. Although for four experiments, T74S1, 74S2, 81S2 and 85S2, the NN alarm occurred prior to the visual observation of smoke, the alarm occurred in each of these cases only after the heating of the combustible was initiated in the presence of diesel emissions. This is in contrast with the optical smoke sensor, SA, which alarmed earlier than the smoke visual observation in seven of the experiments and prior to heating of the combustible in one of the experiments. This shows that the neural network approach with multiple-type fire sensors is more capable of early discriminatory mine

fire detection than an isolated optical path-smoke sensor, the most selective of the fire sensors.

**Sensor correlation.** To measure the effect dilution and dispersion has on a fire signature, the response of fire sensors at S1 and S2 was compared for the same belt fire source in the absence of nuisance emissions, experiments T85S1 and T85S2. Figure 7 shows the correlation, as measured by the covariance of the sensor signals divided by their standard deviations, of the CO sensor signal between stations S1 and S2. The signals are shifted in time due to signature transport, and the signals are diminished due to dilution from the increase in volumetric flow from 3.1 to 4.2 m<sup>3</sup>/s along the air course, and to dispersion over the cross section associated with turbulent airflow.

The correlation between the CO sensors exceeds 0.95 when the CO at S2 has increased less than 2 ppm at 12:03 PM. A

similar correlation analysis applied to the response of MOS sensor, M2, between S1 and S2 showed its long-term correlation was 0.85 after 11:28 AM. When the correlation between two distinct emissions sources, diesel and belt measured CO, was evaluated, only a short time correlation less than 0.7 occurred. This shows the measured time dependent correlation between sensors could be used to determine the uniqueness of the emissions source.

**MOS sensor heating of coal dust.** A persistent condition for coal mines is the presence of coal dust. Because the sensor element for M2 is heated to 250°C (480°F), the exposure of the element to coal dust was a concern. A laboratory evaluation was made of the effect of coal dust on the sensing element of M2. When coal dust with fines less than 0.074 mm was applied directly to an exposed heated element approximately 2 by 3 mm, the effect was an increase in the element's surface resistance, which is characteristic of the response to NO<sub>x</sub> emissions. Neither smoldering nor flaming of the coal dust occurred. When POC from a stick match were made accessible to the dust coated sensing element, the POC penetrated through the coal dust and the sensor's surface element resistance decreased, which is characteristic of a fire response.

**Sensor response to rail torch cutting.** A series of three torch-cutting experiments was conducted in the SRCM to further support the conjecture regarding sensor M2 response for a nuisance event generating NO<sub>x</sub>. In each experiment, a steel rail was cut by an oxygen acetylene torch for approximately four minutes. For these experiments, the CO concentration was relatively low with values between 3.5 and 5.8 ppm above ambient. Smoke sensors, SA and SB, responded with an average signal decrease of 4% and 26%, respectively. These values exceed the ten standard deviation change from their ambient values, which would indicate an alarm value. Sensor M2 response to the lower limit value of zero was indicative of nuisance emissions. Application of the trained neural network to the rail cutting experiments showed the absence of a fire.

## Conclusions

- Coal, conveyor belt and wood mine fire experiments in the presence and absence of diesel emissions determined the optimum multiple sensor type selection for neural network prediction of a fire to be a CO, a POC sensitive MOS, a bimodal NO<sub>x</sub> and POC sensitive MOS sensor, and an optical smoke sensor. The neural network successfully predicted the fire in 22 of 23 cases.
- The ratio of the normalized ionization smoke sensor response to the normalized optical smoke sensor response was shown for coal, conveyor belt and wood fires to be a consistent indicator of a fire in the presence of diesel emissions whenever the ratio exceeded unity, but no earlier a responder than the neural network, and not as definite because of the signal noise.
- In the case of fire emissions' dilution and dispersion between two sensor stations, a time-dependent correlation method successfully identified CO and MOS signatures at two stations as from the same conveyor belt combustion emissions. The correlation method also recognized the difference in CO signatures between diesel and belt emissions from two distinct experiments.
- It was demonstrated with rail burning experiments that a MOS sensor with bimodal response to NO<sub>x</sub> and POC could discriminate the nonfire activity. Application of the neural network analysis verified the rail burning to be a nonfire event.
- A laboratory evaluation demonstrated that coal dust did not smolder nor flame when deposited on a MOS's heated sensor element.

The research conducted with multiple fire sensor types supports their use with a neural network program for mine monitoring to provide a mine fire nuisance-emissions discrimination capability. Incorporation of a trained neural network into a mine monitoring system that included these sensors could provide the coal-mining industry a reliable mine fire detection and nuisance emissions elimination method.

## References

- Brinn, M., and Bott, B., 1994, "A fresh approach to mine fire detection," *The Mining Engineer*, The Institution of Mining Engineers, London, pp. 71-74, Vol. 154, No. 396, Sept. 1994.
- Edwards, J.C., Franks, R.A., Friel, G.F., Lazzara, C.P., and Opferman, J.J., 2001, "Discriminatory mine fire source detection," in *Proceeding of the Seventh International Mine Ventilation Congress*, S. Wasilewski, ed., Cracow, Poland, EMAG publisher, Poland, Ch. 91, pp. 649-655, June 17-22, 2001.
- Edwards, J.C., Franks, R.A., Friel, G.F., Lazzara, C.P., and Opferman, J.J., 2002, "Mine evaluation of discriminating mine fire sensors," in *Proceedings, North American 9th U.S. Mine Ventilation Symposium*, E. DeSouza, ed., Queen's University, Kingston, Ontario, Canada, A.A. Balkema, Lisse, pp. 527-532, June 8-12, 2002.
- Friel, G.F., and Edwards, J.C., 2002, "Neural network application to mine-fire diesel-exhaust discrimination," in *North American/9th U.S. Mine Ventilation Symposium*, E. DeSouza, ed., Queen's University, Kingston, Ontario, Canada, A.A. Balkema publisher, Lisse, pp.533-538, June 8-12, 2002.
- Hambleton, R.T., Clark, R.D.R., Plant, I.J., Walsh, P.T., and P.B. Scott, 1997, "Placement and performance of fire detection equipment in underground mines," *27th International Conference of Safety in Mines Research Institutes*, New Delhi, India, A.A. Balkema, Rotterdam, pp.253-260.
- Ishii, H., Ono, T., Yamauchi, Y., and S. Ohtani, 1994, "Fire detection by multi-layered neural network with delay circuit," *Fire Safety Science - Proceedings of the Fourth International Symposium*, T. Kashiwagi, ed., International Association for Fire Safety Science, Ottawa, July 1994, pp. 761-762.
- Rose-Pehrsson, S.L., Shaffer, R.E., Hart, S.J., Williams, F.W., Gottuk, D.T., Strehlen, B.D., and S.A. Hill, 2000, "Multi-criteria fire detection systems using a probabilistic neural network," *Sensors and Actuators B*, Vol. 69, pp.325-335.
- Code of Federal Regulations, 30 CFR, Parts 75.340 and 75.344, 2001, Office of the Federal Register, National Archives and Standards Administration, U.S. Government Printing Office, Washington, D.C., July 1, 2001.